International Journal of Thin Film Science and Technology

Volume 9
Issue 1 *Jan. 2020*

Article 9

2020

Enhanced Activity of Chemically Synthesized Nanorod Mn3O4 Thin Films for High Performance Supercapacitors

P. Immanuel
Department of Physics, National Changhua University of Education, Changhua 500, Taiwan., kodaiimmanuvel@gmail.com

G. Senguttuvan
Department of Physics, University College of Engineering- BIT campus, Anna University, Tiruchirappalli, India, kodaiimmanuvel@gmail.com

K. Mohanraj
Raman Research Laboratory, PG & Research Department of Physics, Government Arts College, Tiruvannamalai-606603, Tamilnadu, India\\ Department of Physics Graduate Institute of Photonics, National Changhua University of Education, Changhua 500, Taiwan., kodaiimmanuvel@gmail.com

International Journal of Thin Films Science and Technology

http://dx.doi.org/10.18576/ijtfst/090109

Enhanced Activity of Chemically Synthesized Nanorod Mn_3O_4 Thin Films for High Performance Supercapacitors

P. Immanuel[1*], *G. Senguttuvan*[2] *and K. Mohanraj*[3, 4]

[1]Department of Physics, National Changhua University of Education, Changhua 500, Taiwan.

[2]Department of Physics, University College of Engineering- BIT campus, Anna University, Tiruchirappalli, India

[3]Raman Research Laboratory, PG & Research Department of Physics, Government Arts College, Tiruvannamalai-606603, Tamilnadu, India

[4]Department of Physics Graduate Institute of Photonics, National Changhua University of Education, Changhua 500, Taiwan.

Received: 26 Aug. 2019, Revised: 10 Nov. 2019, Accepted: 20 Nov. 2019

Published online: 1 Jan. 2020

Abstract: The present study addresses a cost effective method for fabricating high performance and flexible supercapacitor based on the transition metel oxides of Mn_3O_4 thin films. The Mn3O4 prepared by SILAR method at different cycles such as 25, 50, 75 and 100 cycles. The prepared Mn_3O_4 thin films were characterized by means of structural, morphological and electrochemical studies. The structural studies of X-ray diffraction (XRD) reveal that 75 cycles have good crystalline nature with tetrahedral structure. Fourier transform infrared spectroscopy (FTIR) indicates the functional group of Mn-O. Raman spectra indicate the formation of Mn_3O_4 thin films. SEM analysis depicted that Mn_3O_4 thin films have a rod-like structure. TEM images show the SAED pattern and lattice fringes of Mn_3O_4. The electrochemical measurements of CV, GCD and impedance measurements are investigated using 1M Na2SO4 electrolyte. In the electrochemical measurement Mn_3O_4 thin films exhibit the maximum specific capacitance value of 295 Fg^{-1} at the scan rate of 2 mVs^{-1}.

Keywords: Thin films, Supercapacitor, Mn3O4, Cyclic Voltammetry, SILAR.

1 Introduction

In the current situation, energy storage devices are more important in the field of rapid development of the nation. Developing social process requires energy storage and replacing the other storage devices like a battery. Also, converting the alternative energy storage is critical. Supercapacitors have a long life cycle, high power density and very good reversibility. Transition metal oxide has a main role in the energy storage devices used as one of electrode materials, including RuO [1], MnO [2], V_2O_5 [3], Iron [4], Cobalt [5], Nickle [6], …etc. MnO is a promising electrode material, eco-friendly, non-toxic and cost-effective. Preparation of Mn_3O_4 involves various method, such as spray pyrolysis [7], sol-gel [8], hydrothermal method [9], Physics vapour deposition [10], thermal decomposition [11] and SILAR [12]. Successive ion layer adsorption and reaction (SILAR) method is suitable for the film's preparation because of its easy preparation, uniform coating, controlling thickness and low cost. Girishgund et al, [13] prepared pure Mn_3O_4 and composite thin films using it. Dubal et al, [14] reported the maximum specific capacitance value of 314 Fg^{-1} using the same method. Zhenghua Su et al, [15] prepared sulfurizing stacked thin films utilizing it. It is the most suitable method for the preparation of thin films.

In the present work focused on the Mn_3O_4 thin films prepared at different cycles such as 25, 50, 75 and 100 using a simple and inexpensive successive ionic layer and adsorption method. The manganese oxide is well deposited on the substrate and the results are investigated by structural, morphological and electrochemical studies.

2 Experimental Procedures

The Mn_3O_4 thin films were prepared using SILAR method. The substance was used as a well-cleaned glass substrate and stainless steel mesh (SS). Analytical grade of MnSo4 (0.1 M) and NaOH (0.1 M) was used as a precursor, First, Mn_3O_4 was dissolved in 100 ml of double distilled water (DDW) used as a cationic solution and the anions solution

*Corresponding author E-mail: kodaiimmanuvel@gmail.com

of NaOH was dissolved in 100 ml of DDW. The schematic diagram of SILAR method is presented in Fig.1.

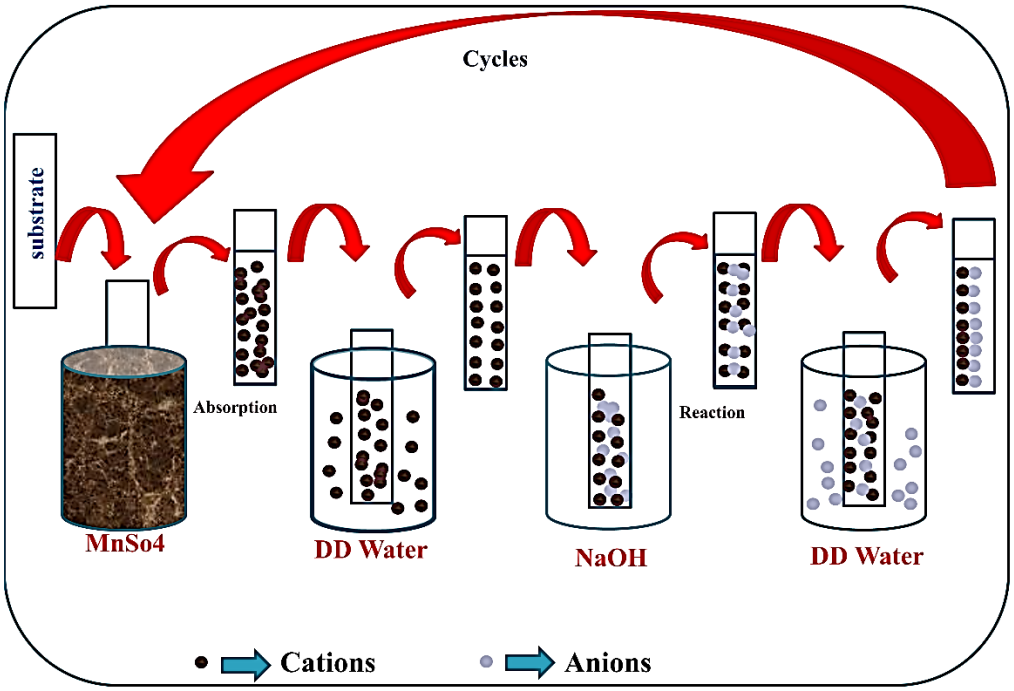

Fig.1: Schematic diagram of SILAR method.

Table.1: Optimised parameters of prepared Mn_3O_4 Thin films.

S. No.	Parameters		
1	Precursor solution	$MnSO_4$ (cation)	NaOH (anion)
2	Concentration (M)	0.1	1
3	Immersion time (sec)	20	20
4	Rinsing time (sec)	10	10
5	Temperature (Kelvin)	273	273

The figure indicates the formation of Mn_3O_4 thin films. The cationic and anionic solution was kept in a beaker 1, 3 and 2, 4 filled with the DDW. The well-cleaned glass and SS substrates are immersed in the cationic solution. The substrates adsorbed the Mn ions in 20 sec and dried at air atmosphere 5 sec. Then, they were dipped in DDW again to remove the loosely bounded Mn ions. Yet again the substrate were immersed in the anionic solution to absorb the OH- ions and reacted with the Mn ion in 20 sec and dried at air atmosphere 5 sec. Then, it was dipped in the DDW to remove the unreacted ions in the process like one cycle. The cycles varied from 25 to 100 cycles in the step of 25 cycles. The cycle's film thickness and properties of Mn_3O_4 thin films may change.

2.1 Film Characterization

An X-ray diffractometer (XRD) system "6000 Shimadzu X-ray diffractometer" using CuKa radiation with λ=0.1541 nm was used to identify the crystal structures of the films. The Fourier transform infrared (FTIR) spectra are carried out using the model JASCO 4600. Raman spectra were carried out in the range of 100-1000 cm^{-1} using the Jobin-Yvon T64000 Raman scattering system with an Olympus microscope equipped with a 100-magnification lens in backscattered configuration. A Scanning Electron

Microscope (SEM) images are used to find the morphology of the prepared Mn_3O_4 thin film with VEGA3 TESCAN model and EDAX analysis by Bruker Nano Gmbh, Germany. The morphologies and SAED pattern of the manganese oxide were observed on the High-Resolution Transmission Electron Microscope (HR-TEM) analysis (Model of the instrument FEI –TECNAI G2-20 TWIN 200kV with LaB6 filament with an acceleration voltage of 200 kV).

2.2 Electrochemical Measurements

The electrochemical measurement was investigated using CHI 760 D electrochemical work station. All the electrochemical measurements were analysed by the three electrodes: 1. Mn_3O_4 is s a working electrode, 2. SCD is the reference electrode, and 3. Platinum wire as the counter electrode. 1 M of Na_2SO_4 solution was used as an electrolyte. This work station was used to investigate the CV, GCD and electrochemical impedance measurement. CV measurements are carried in the different scan rate 2 mVs^{-1} to 100 mVs^{-1}, and the CV performed a potential window -0.2 to 1.0 V. The GCD studies were conducted at the current density of 2 mA within the potential window -0.2 to +1.0 V. Electrochemical impedance measurement was investigated between the 0.01Hz and 100 kHz with AC amplitude of 100 mV.

3 Results and Discussion

3.1 Structural Studies

The XRD pattern shows the cycle's variation of Mn_3O_4 thin films. The cycles from 25, 50, 75 and 100 cycles. It reveals 25 cycles with amorphous nature. Cycling intensity of the peaks gradually increases because the Mn ions are uniformly deposited on the lattice**.** The XRD Pattern of Mn_3O_4 thin films indicates that the corresponding peaks are (101), (112), (200), (103), (211), (220), and (215) planes which are consistent with the Girish at al [13]. They are assigned to the tetragonal hausmannite structure. The values are compatible with the standard JCPDS card number 24-0734. Manganese oxide has a different structure. Properties of Mn ions $Mn^{2+,}$ Mn^{3+} and Mn^{4+} in the positions of manganese oxides are MnO, MnO_2, Mn_2O_3 and Mn_3O_4. The well-stabled Mn_3O_4 thin films are prepared at room temperature. They have stable spinel oxide in 273 K. Mn^{2+} and Mn^{3+} ions are located at the tetrahedral and octahedral sites. Tetrahedral sites are surrounded by four oxygen ions, but octahedral sites are surrounded by six oxygen ions [16].

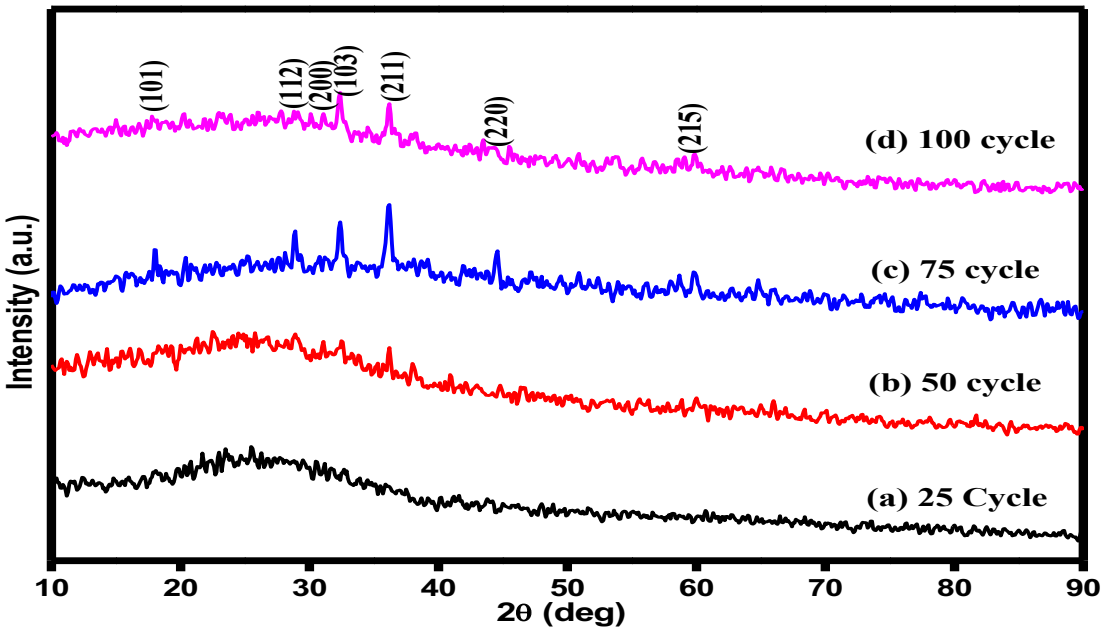

Fig.2: XRD pattern of Mn_3O_4 thin films.

The average crystallite size of Mn_3O_4 thin films was calculated using the Debye Scherer's equation [17],

$$D = \frac{K\lambda}{\beta \cos\theta} \quad (1)$$

Where k is the shape factor (0.9), λ is the wavelength of the X- ray, β is full with and half maxima, and θ is the angle of the diffraction. Dislocation density (δ) and microstrain (ε) also calculated [18]. Dislocation density is defined as the length of dislocation lines per unit volume of the crystalline material. The calculated results are presented in Table 2. Dislocation density and microstrain was calculated from the following equation (2) and (3):

$$\delta = \frac{1}{D2} \quad (2)$$

$$\varepsilon = \frac{\beta \cos\theta}{4} \quad (3)$$

3.2 Thickness Measurement

Thickness measurement was carried out from gravimetric weight difference method with the relation t=M/1000 x density x area, where t is thickness, m is the mass of the film deposited on the substrate in milligram, A is area of the deposited film in cm^2, density of the deposited materials (=7.21 gcm^{-3}) is in bulk form. Fig.2 indicates that when the number of cycles like 25, 50, 75 and 100 increases, film thickness gradually increases. P.M Kulal et al [19], using thin films prepared by the chemical deposition from the gravimetric weight difference method. A.Abhijt et al [20] prepared, using spray pyrolysis method, thin films to define thickness in weight difference method. Increasing the deposition cycles 25 to 100 in the steps of 25, thickness of the film increases to 0.48, 0.61, 0.98 and 1.35 µm.

3.3 FTIR and Raman Studies

FTIR Spectrum shows the cycle's variation of Mn_3O_4 thin films ranging from 400 - 4000 cm^{-1}. The bands 615 cm^{-1} attributed the stretching modes of Mn-O in tetrahedral sides and 499 cm^{-1} corresponding to the Mn-O bands in octahedral sides. The bands of 3746 and 1544 cm^{-1} are assigned to the stretching and bending vibration of –OH molecules. This results conforms to the formation of Mn_3O_4 thin films. The Raman spectra of pure Mn_3O_4 thin films are presented in the Fig.4. The Raman studies indicate the dominant peak of 655 cm^{-1} assigned the vibrational mode of Mn_3O_4. Qu. jiangying et al. [21] reported the Raman spectrum and observed the Mn_3O_4 peak at 652 cm^{-1}. The peak is the evidence of the presence of Mn_3O_4 thin films. It has a spinel structure corresponding to the Mn-O vibrations. Anilkumar et al. [22] reported the specific vibrations of pure Mn_3O_4 at 640 cm^{-1}.

Table. 2: Structural parameters of Mn_3O_4 Thin films.

S. No.	Cycles	Crystallite size D (nm)	Dislocation density (δ) $X10^{-12}$ m^{-2}	Micro strain (ε) $X10^{-3}$
1	50	13	5.91	2.53
2	75	9	12.34	3.70
3	100	11	8.26	3.19

The Raman spectra of the film exhibit highest intensity peak is 655 cm^{-1}. Hui xial et al. [23] observed 652.1 cm^{-1} and Larbi et al. observed [24] 655 cm^{-1}indicating good agreement with the reported value. The intense vibrational mode located at 653 cm^{-1}. Julienetal et al. [25] reported the characteristic of Mn_3O_4 with the spinel structure corresponding to the Mn-O breathing vibrations of Mn^{2+} ions. Kim et al. [26] reported that Mn^{2+} is located in the tetrahedral coordination.

3.4 SEM and TEM

The surface morphology of 50 (A), 75 (B), and 100 (C) cycle Mn_3O_4 thin films is presented in Fig.5. The SEM the gravimetric weight difference method to measure film thickness in SILAR method, reported that the values increased when the number of cycles increased. D.P.Dubal et al [14] reported and calculated thickness of the Mn_3O_4 image indicates Mn_3O_4 thin films with a rod-like structure. Increasing the number of the cycle in the step of 25 cycles improved the surface morphology. The improved morphology shows the rod-like structure. Fig.5 (A) indicates the smooth surface, 75 and 100 cycles indicates the improved nanorods. Mn_3O_4 nanorods resemble a bundle of grass and it is presented in Fig 5 (B). The length of the rod is around 3.12 µm. Presence of Mn and O is conformed to the EDAX analysis presented in the Fig.5 (D). Fig.6 reveals the pristine Mn_3O_4 TEM images as prepared by 75 cycles. TEM indicates the nanorod-like structure. SAED pattern is consistent with the XRD results. The observed lattice fringes with d-spacing of ~ 0.26 nm correspond to the high intense plane of XRD confirming the tetragonal phase structure of Mn_3O_4. Mn and O are conformed with EDAX.

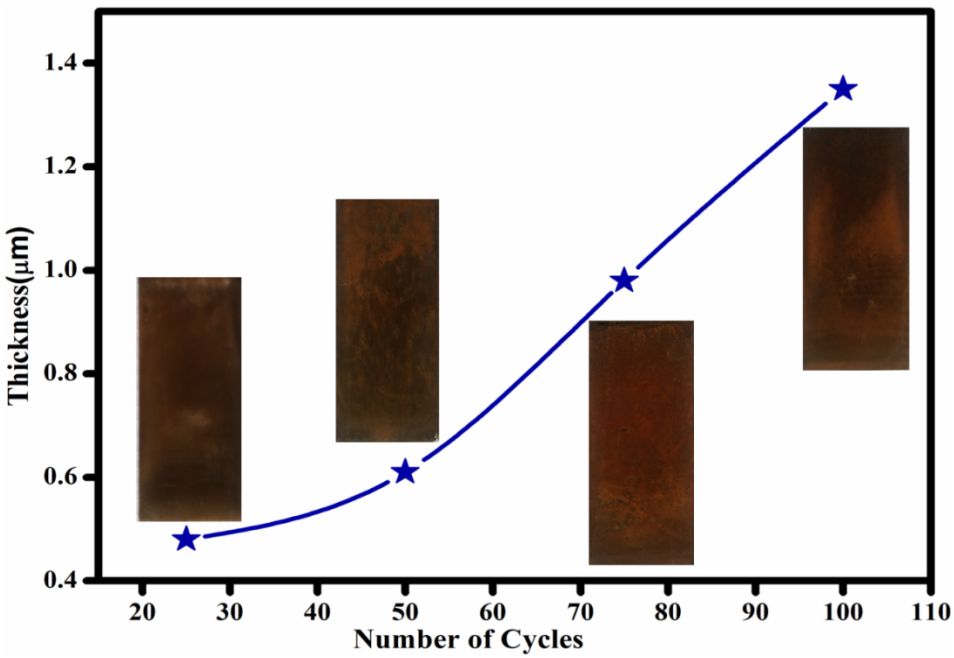

Fig.3 :Thickness measurement of Mn_3O_4 thin films.

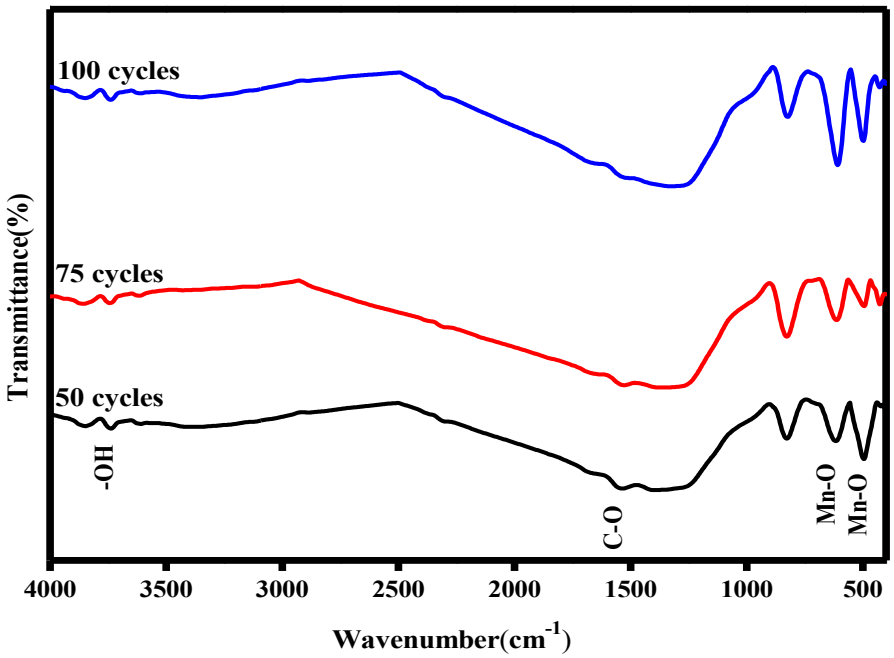

Fig.4 :FTIR spectrum of Mn_3O_4 thin films.

Electrochemical studies were carried out by 75 and 100 cycles. CV, GCD and impedance studies investigated the electrochemical properties of Mn_3O_4 thin film electrode using three-electrode system. Figures 8 and 9 indicate the CV curve which was carried out by different scan rate 2 to 100 mVs^{-1}. All CV curves resembles a quasi-rectangular shape. These curves reveal their ideal capacitance nature [21]. In this process, increase the scan rate increases from 2 mVs^{-1} to100 mVs^{-1}. The anodic and catholic peaks shift from positive to negative potential. There is less diffusion of negative materials at high scan rate. The anodic peak indicates the oxidation process of the electrode material and cathodic peak reveals the reduction process.

The specific capacitance value was calculated using the equation (5)

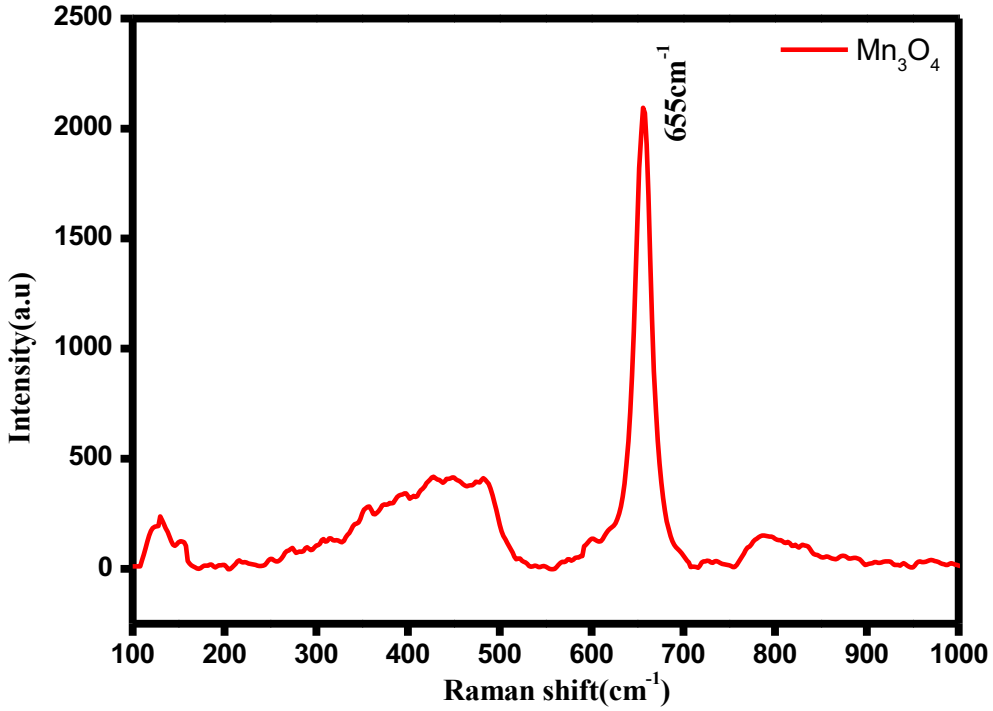

Fig.5: Raman spectrum of Mn_3O_4 thin films.

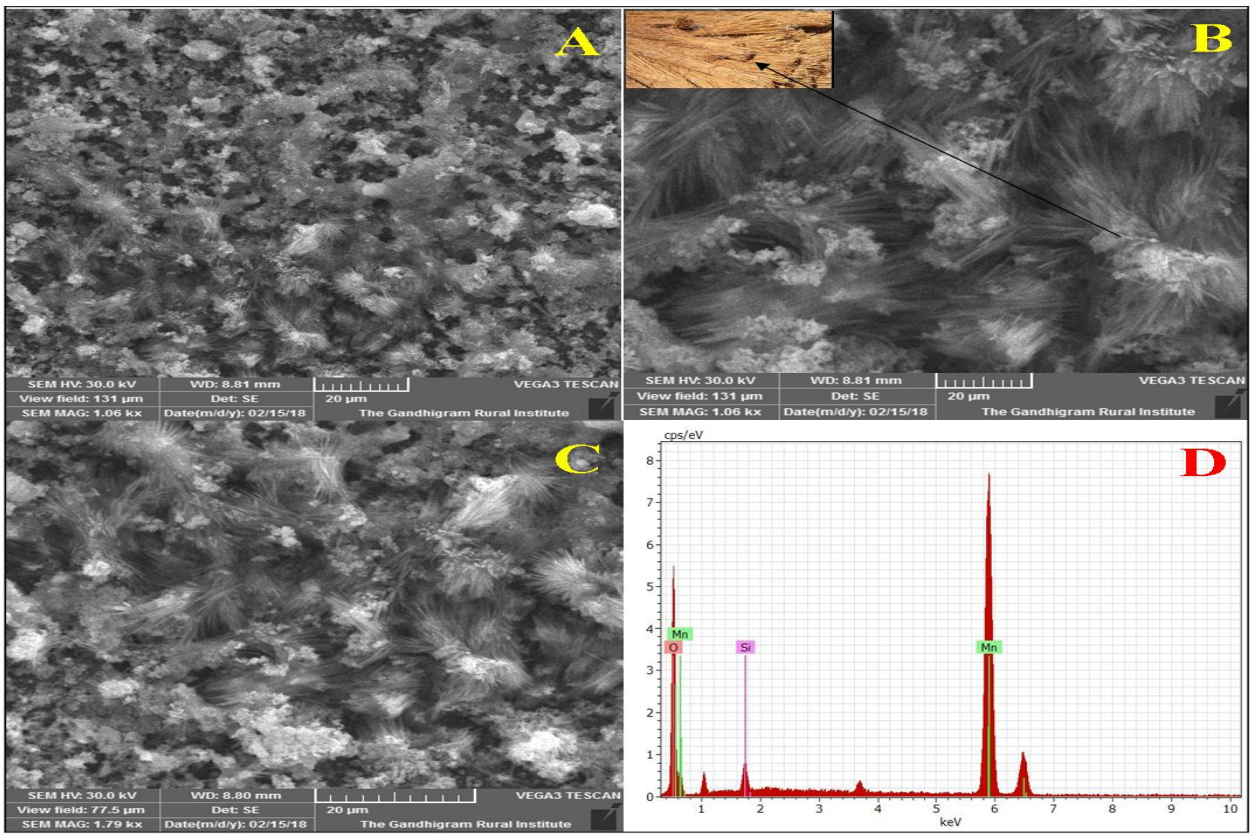

Fig.6: SEM images of Mn_3O_4 thin films.

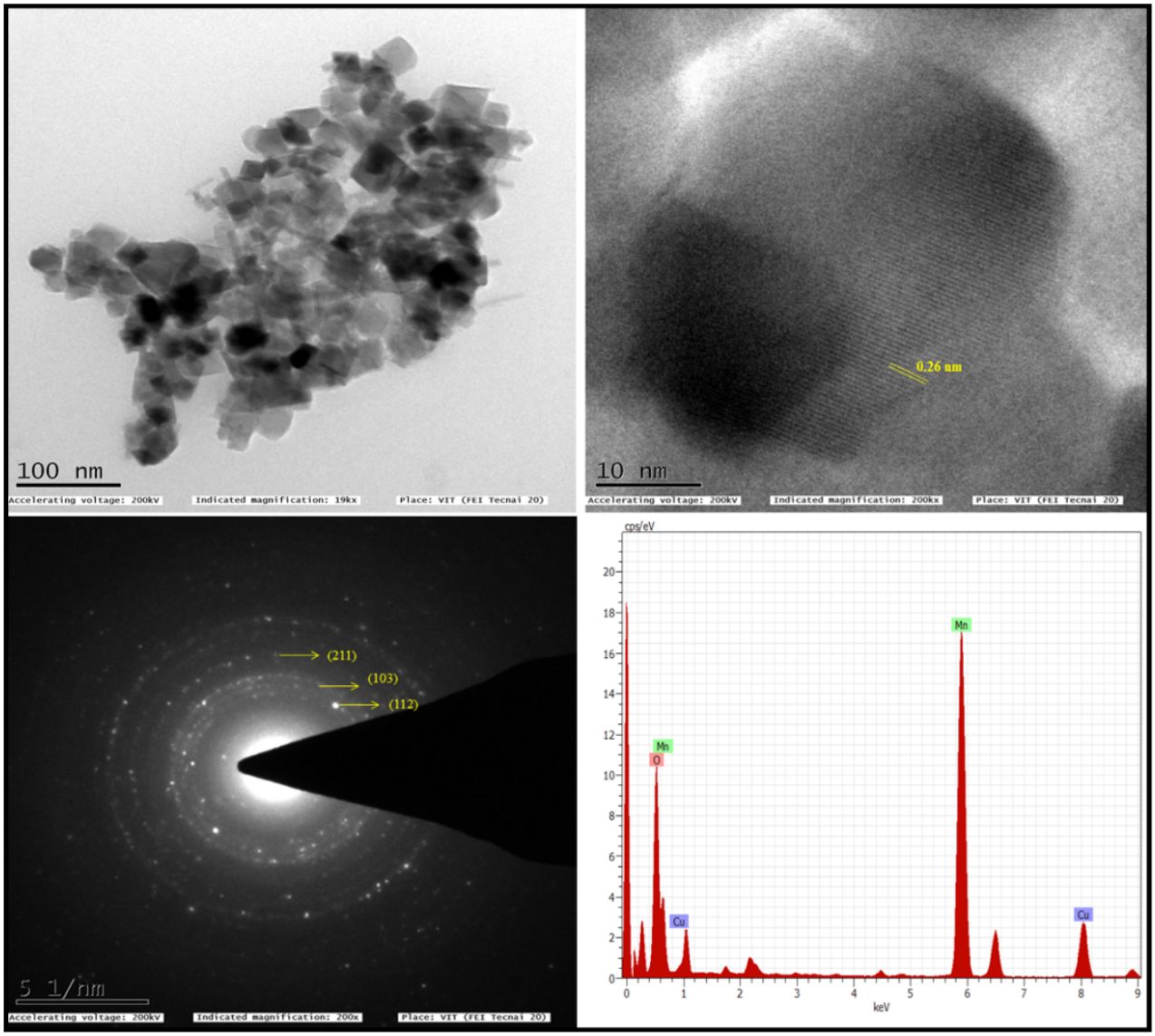

Fig.7:TEM images of Mn_3O_4 thin films.

$$C = \frac{Imax}{w\ X\left(\frac{dv}{dt}\right)} \quad (4)$$

$$C = \frac{I\ X\ \Delta t}{m\ X\ \Delta V} \quad (5)$$

The CV measurement of 75 cycles shows the specific capacitance value in the scan rate of 2, 5, 10, 20, 40, 60, 80 and 100 mVs^{-1}. The specific capacitance values are 295,160, 80, 52, 30, 20, 10 and 5 Fg^{-1} and 100 cycles have a 167, 90, 65, 52,33,22,15 and 7 Fg^{-1}. Increasing the scan rate decreases the specific capacitance value decreasing because the highest scan rates is assigned to the presence of inner active sites that cannot sustain the redox transitions which occurs due to the diffusion effect of ions with the electrode. The GCD curves carried out pure Mn_3O_4 thin films electrodes in 1 M Na_2SO_4 at 2 mA cm^{-1} current density and potential range from -0.3 to 0,8 V/SCE. The galvanostatic charge-discharge curve is presented in Figure 10. It also exhibits the potential drop. The specific capacitance values are calculated using the relation (5):

Where I is the current density, Δt is the discharge time, m represents the mass of the material, ΔV indicates the potential window. The specific capacitance value calculated 75 and 100 cycles of Mn_3O_4 electrode. The specific capacitance values are 180 and 100 Fg^{-1} for the current density 2 mA. Compared to these cycles, 75 cycles have a good specific capacitance value. The electrochemical impedance spectra (EIS) were measured in the open circuit potential at the alternative current of 2 mV. Fig.11 shows Nyquist plot which is composed to the semi-circle at high frequency range in high. After that line, nearly a straight line at a low and high frequency represents the ion diffusion and charge transfer resistance. The symmetry of the specific capacitance values is presented in Table.3.

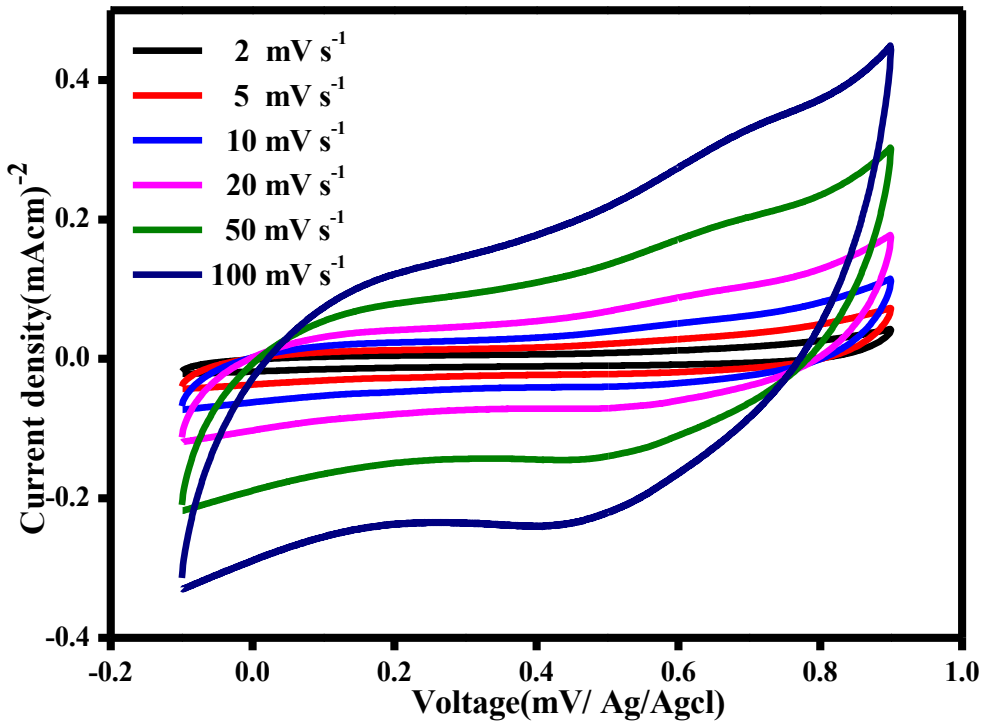

Fig.8. CV curve of 75 cycles Mn_3O_4 thin films with a different scan rate.

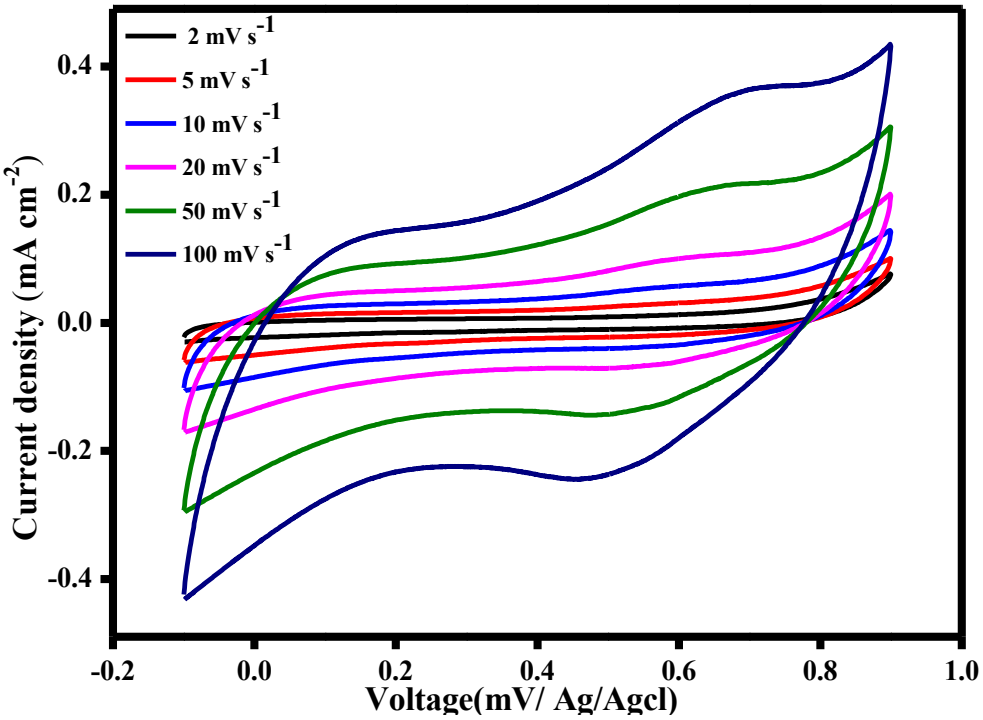

Fig.9. CV curve of 100 cycles Mn_3O_4 thin films with different scan rate.

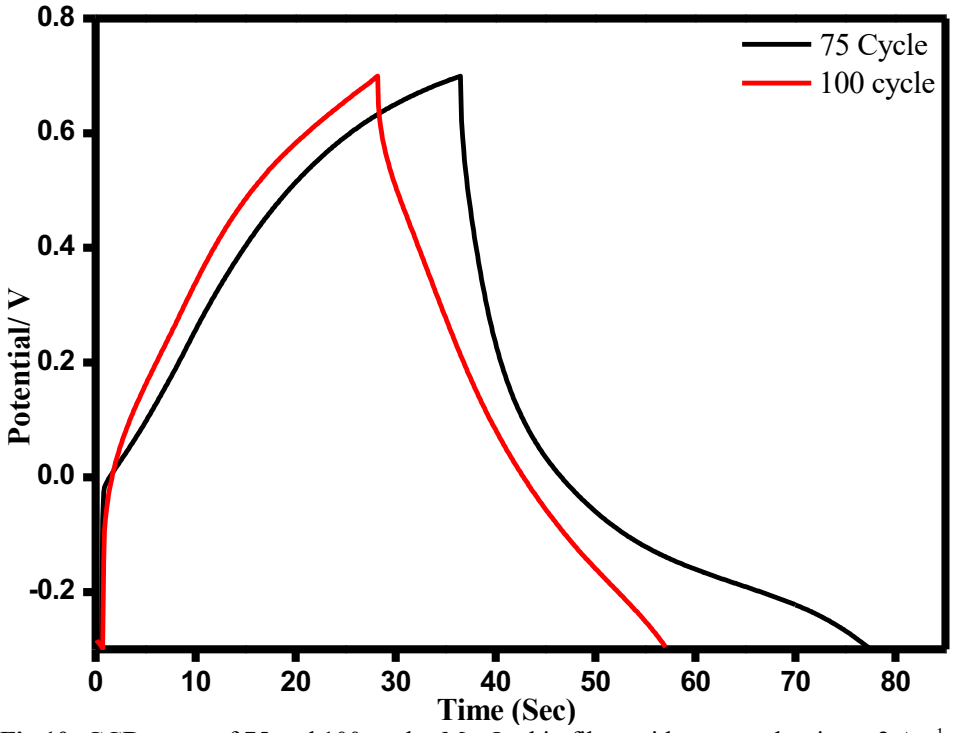

Fig.10: GCD curve of 75 and 100 cycles Mn_3O_4 thin films with current density at 2 Ag^{-1}.

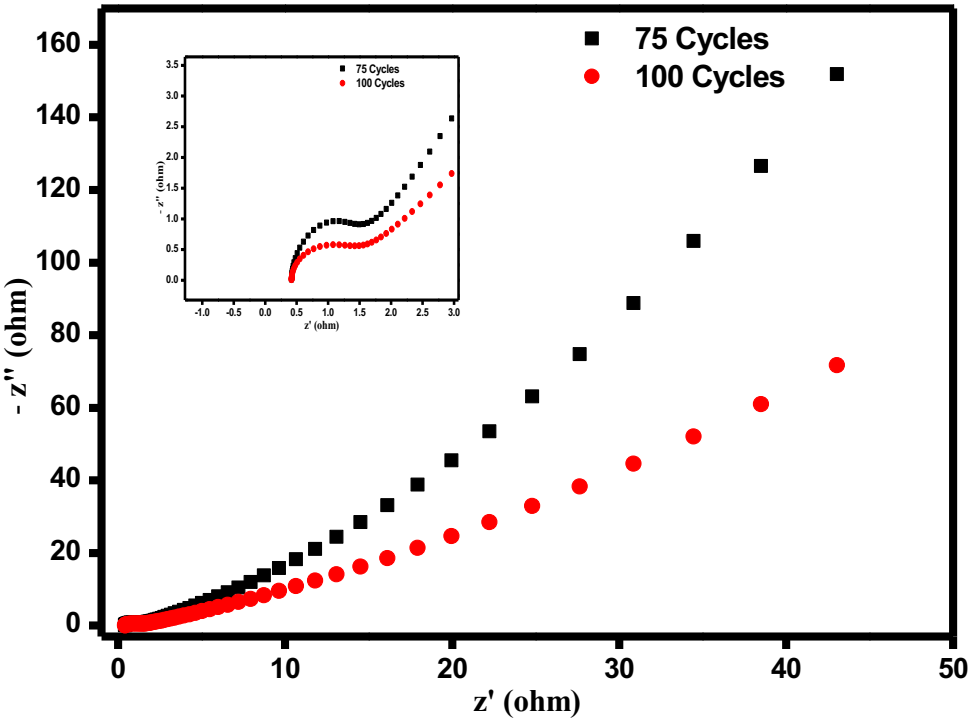

Fig.11: Nyquist plot 75 and 100 cycles Mn_3O_4 electrodes in the frequency range of 0.01Hz to 100 KHz in 1M Na_2SO_4.

Table 3: Electrochemical performance of Mn_3O_4 electrode material in three electrode system.

Electrode Materials	Electrolyte	Scan rate	Capacitance (Fg^{-1})	Ref
Mn_3O_4	1 M Na_2SO_4	5 MvS^{-1}	144 Fg^{-1}	[22]
Mn_3O_4	1 M Na_2SO_4	5 MvS^{-1}	258	[27]
Mn_3O_4	1 M Na_2SO_4	5 MvS^{-1}	175	[28]
Mn_3O_4	1 M Na_2SO_4	5 MvS^{-1}	234 Fg^{-1}	[29]
Mn_3O_4	1 M Na_2SO_4	10MvS^{-1}	160 Fg^{-1}	[30]
Mn_3O_4	1 M Na_2SO_4	10 MvS^{-1}	193 Fg^{-1}	[12]
Mn_3O_4	1 M Na_2SO_4	2 MvS^{-1}	295 Fg^{-1}	**Present work**

4 Conclusions

Mn_3O_4 thin films were prepared using the simple and inexpensive SILAR method. The films prepared by different cycles vary from 25 to 100 cycles in the step of 25. The cycle 75 is the optimal cycle. XRD results confirm that the formation of Mn_3O_4 thin films has polycrystalline nature with tetrahedral structure. FTIR studies indicate the chemical bounding of Mn and Oxygen. Raman spectra exhibit that formation of Mn_3O_4 thin films. SEM studies indicate that the 75 cycles have a nanorod structure resembling a bundle of gross. Compared to the other deposition cycles, 75 cycles present a good result. TEM images indicate that SAED pattern is consistent with XRD planes. Lattice fringes with d-spacing of ~ 0.26 nm correspond to the high intense plane of XRD confirming the tetragonal phase structure of Mn_3O_4. The electrochemical measurements, i.e. CV, GCD and impedance measurements, are investigated using the 1M Na_2SO_4 electrolyte. In the electrochemical measurement, 75 cycles deposited Mn_3O_4 thin films exhibit the maximum specific capacitance value of 295 Fg^{-1} at the scan rate of 2 mVs^{-1}.

References

[1] K. Brousse, S. Nguyen, A. Gillet, S. Pinaud, R. Tan, A. Meffre, K. Soulantica, B. Chaudret, P.L. Taberna, M. Respaud, P. Simon, Laser-scribed Ru organometallic complex for the preparation of RuO2 micro-supercapacitor electrodes on flexible substrate, Electrochim. Acta., 2018.

[2] W. Xu, Z. Jiang, Q. Yang, W. Huo, M.S. Javed, Y. Li, L. Huang, X. Gu, C. Hu, Approaching the lithium-manganese high-performance supercapacitor, Nano Energy., **43**, 168–176, 2018.

[3] L.-L. Xing, G.-G. Zhao, K.-J. Huang, X. Wu, A yolk-shell V2O5 structure assembled from ultrathin nanosheets and coralline-shaped carbon as advanced electrodes for a high-performance asymmetric supercapacitor., Dalton Trans., **47** 2256–2265., 2018.

[4] J. Luo, Z. Zheng, A. Kumamoto, W.I. Unah, S. Yan, Y.H. Ikuhara, X. Xiang, X. Zu, W. Zhou, PEDOT coated iron phosphide nanorod arrays as high-performance supercapacitor negative electrodes, Chem. Commun., **54** 794–797, 2018.

[5] K.V. Sankar, S.C. Lee, Y. Seo, C. Ray, S. Liu, A. Kundu, S.C. Jun, Binder-free cobalt phosphate one-dimensional nanograsses as ultrahigh-performance cathode material for hybrid supercapacitor applications, J. Power Sources., **373** 211–219, 2018.

[6] N. Parveen, S.A. Ansari, S.G. Ansari, H. Fouad, N.M. Abd El-Salam, M.H. Cho, Solid-state symmetrical supercapacitor based on hierarchical flower-like nickel sulfide with shape-controlled morphological evolution, Electrochim. Acta., **268** 82–93, 2018.

[7] R.C. Ambare, B.J. Lokhande, Solution concentration and decomposition temperature dependent electrochemical behavior of aqueous route spray pyrolysed Mn3O4: supercapacitive approach, J. Mater. Sci. Mater. Electron., **28** 12246–12252, 2017.

[8] C.-K. Lin, K.-H. Chuang, C.-Y. Lin, C.-Y. Tsay, C.-Y. Chen, Manganese oxide films prepared by sol–gel process for supercapacitor application, Surf. Coatings Technol., **202** 1272–1276, 2007.

[9] H.U. Shah, F. Wang, A.M. Toufiq, S. Ali, Z.U.H. Khan, Y. Li, J. Hu, K. He, Electrochemical Properties of Controlled Size Mn 3 O 4 Nanoparticles for Supercapacitor Applications, J. Nanosci. Nanotechnol., **18**, 719–724, 2018.

[10] Y.Q. Chang, X.Y. Xu, X.H. Luo, C.P. Chen, D.P. Yu, Synthesis and characterization of Mn3O4 nanoparticles, J. Cryst. Growth., **264**, 232–236, 2004.

[11] X. Shen, Z. Ji, H. Miao, J. Yang, K. Chen, Hydrothermal synthesis of MnCO3 nanorods and their thermal transformation into Mn2O3 and Mn3O4 nanorods with single crystalline structure, J. Alloys Compd. **509**, 5672–5676, 2011.

[12] D.P.Dubal, D.S.Dhawale, R.R.Salunkhe, S.M.Pawar, C.D.Lokhande, A novel chemical synthesis and characterization of Mn3O4 thin films for supercapacitor application, Appl. Surf. Sci., **256**, 4411-4416, 2010.

[13] G.S. Gund, D.P. Dubal, B.H. Patil, S.S. Shinde, C.D. Lokhande, Enhanced activity of chemically synthesized hybrid graphene oxide/Mn3O4composite for high performance supercapacitors, Electrochim. Acta., **92**, 205–215, 2013.

[14] D.P. Dubal, D.S. Dhawale, R.R. Salunkhe, V.J. Fulari, C.D. Lokhande, Chemical synthesis and characterization of Mn3O4 thin films for supercapacitor application, J. Alloys Compd., **497**, 166–170, 2010.

[15] Z. Su, C. Yan, K. Sun, Z. Han, F. Liu, J. Liu, Y. Lai, J. Li, Y. Liu, Preparation of Cu2ZnSnS4thin films by sulfurizing stacked precursor thin films via successive ionic layer adsorption and reaction method, Appl. Surf. Sci., **258**, 7678–7682, 2012.

[16] F. Wang, H. Wu, Z. Lin, S. Han, D. Wang, Y. Xue, Y. Sun, J. Sun, B. Li, Shape evolution of Cu-doped Mn3O4 spinel microcrystals: influence of copper content, Mater. Res. Bull., **45**, 1567–1573, 2010.

[17] F. Yang, M. Zhao, Q. Sun, Y. Qiao, A novel hydrothermal synthesis and characterisation of porous Mn 3 O 4 for supercapacitors with high rate capability, RSC Adv., **5** 9843–9847, 2015.

[18] P. Immanuel, A. Prakash, C.R. Mohan, Ethanol sensing of V2O5 thin film prepared by spray pyrolysis technique: Effect of substrate to nozzle distance, in: AIP Conf. Proc., AIP Publishing LLC., 80022, 2017.

[19] P.M. Kulal, D.P. Dubal, C.D. Lokhande, V.J. Fulari, Chemical synthesis of Fe2O3 thin films for supercapacitor application, J. Alloys Compd., **509**, 2567–2571, 2011.

[20] A.A. Yadav, S.N. Jadhav, D.M. Chougule, P.D. Patil, U.J. Chavan, Y.D. Kolekar, Spray deposited Hausmannite Mn3O4thin films using aqueous/organic solvent mixture for supercapacitor applications, Electrochim. Acta. 206, 134–142, 2016.

[21] Q. Jiangying, G. Feng, Z. Quan, W. Zhiyu, H. Han, L. Beibei, W. Wubo, W. Xuzhen, Q. Jieshan, Highly atom-economic synthesis of graphene/Mn3O4 hybrid composites for electrochemical supercapacitors, Nanoscale., **5**, 2999, 2013.

[22] M. Anilkumar, V. Ravi, Synthesis of nanocrystalline Mn3O4 at 100 °C, Mater. Res. Bull., **40**, 605–609, 2005.

[23] H. Xia, Y. Wan, F. Yan, L. Lu, Manganese oxide thin films prepared by pulsed laser deposition for thin film microbatteries, Mater. Chem. Phys., **143**, 720–727, 2014.

[24] T. Larbi, A. Amara, L. Ben Said, B. Ouni, M. Haj Lakhdar, M. Amlouk, A study of optothermal and AC impedance properties of Cr-doped Mn<inf>3</inf>O<inf>4</inf> sprayed thin films, Mater. Res. Bull., **70**, 254–262, 2015.

[25] C.. Julien, M. Massot, C. Poinsignon, Lattice vibrations of manganese oxides: Part I. Periodic structures, Spectrochim. Acta Part A Mol. Biomol. Spectrosc., **60**, 689–700, 2004.

[26] M. Kim, X.M. Chen, X. Wang, C.S. Nelson, R. Budakian, P. Abbamonte, S.L. Cooper, Pressure and field tuning the magnetostructural phases of Mn 3 O 4 : Raman scattering and x-ray diffraction studies, Phys. Rev. **B. 84** 174424, 2011.

[27] M. Aghazadeh, A. Bahrami-Samani, D. Gharailou, M.G. Maragheh, M.R. Ganjali, P. Norouzi, Mn3O4 nanorods with secondary plate-like nanostructures; preparation, characterization and application as high performance electrode material in supercapacitors, J. Mater. Sci. Mater. Electron., **27**, 11192–11200, 2014.

[28] B. Wang, J. Park, C. Wang, H. Ahn, G. Wang, Mn3O4 nanoparticles embedded into graphene nanosheets: Preparation, characterization, and electrochemical properties for supercapacitors, Electrochim. Acta., **55**, 6812–6817, 2010.

[29] M. Aghazadeh, M.R. Ganjali, P. Norouzi, Preparation of Mn 5 O 8 and Mn3O4 nano-rods through cathodic electrochemical deposition-heat treatment (CED-HT), Mater. Res. Express., **3**, 55013, 2016.

[30] S. Zhao, T. Liu, Y. Zhang, W. Zeng, T. Li, S. Hussain, D. Hou, X. Peng, Cr-doped MnO2 nanostructure: morphology evolution and electrochemical properties, J. Mater. Sci. Mater. Electron., **27**, 3265–3270, 2016.